

THE CONTINUOUS SPECTRUM OF NEUTRAL HELIUM FROM GASEOUS NEBULAE*

J. B. KALER

University of Illinois Observatory

P. LEE

Louisiana State University

AND

L. H. ALLER

University of California, Los Angeles

Received 1970 February 17; revised 1970 June 29

ABSTRACT

We have detected the continuous spectrum associated with the 2^3P term of neutral helium in six planetary nebulae and the Orion Nebula. Although the errors are large, we are able to make reasonable estimates of the strength of this continuum in most of these nebulae. On the average, the ratio of the flux density of the 2^3P continuum to the flux in the $\lambda 4471$ line of He I is about twice as great as that predicted by recombination theory at the electron temperature measured from the forbidden lines. In addition, the ratio of the flux density of the 2^3P continuum to that of the Balmer continuum is generally significantly greater than is allowed on the basis of the measured helium-to-hydrogen ratio.

I. INTRODUCTION

The observed continua of gaseous nebulae consist of three main components (if one excludes scattering from dust): the two-quantum, the free-free, and the bound-free continua of hydrogen (see, e.g., Aller 1956). The abundances of the other elements are so low compared with hydrogen that their continua are generally exceedingly weak. We report here on the observation of another component, the recombination continuum to the 2^3P term of neutral helium. We can identify this feature in the spectra of the planetary nebulae NGC 6572, NGC 6543, IC 4997, and IC 418, and in the spectrum of the Orion Nebula. A more tentative identification can be made for NGC 7009 and NGC 7662. Menzel (private communication) appears to have observed this continuum in the spectrum of NGC 6543 on a plate taken with the Crossley reflector in about 1930.

Bethe (1964) gives the energy of the 2^3S_1 level of neutral helium as 0.35047 rydbergs. If we combine this figure with the energy of the 2^3P-2^3S transition (at 10830 Å), we find that the low energy limit of the continuum lies at 3421.5 Å, which corresponds to the 2^3P-n^3D , 2^3P-n^3S series limits. In actual practice, we would expect the *apparent* series limit to be somewhat longward of $\lambda 3421.5$ due to the blending of the lines with high n , which is in fact what we find.

The 2^3P-n^3S series has been extensively observed in gaseous nebulae. For example, Aller and Kaler (1964*a*) extend the series to nearly $n = 20$ for NGC 7009. These helium lines (as well as those of the 2^1P-n^1D series) have intensities which, when compared with the intensity of $\lambda 4471$ (2^3P-4^3D), are often found to be considerably stronger than predicted by theory at the temperature measured from the forbidden lines (Kaler 1966). It is consequently of interest to measure the intensity of the 2^3P continuum to see whether it shares the above anomaly with the lines, as does the hydrogen continuum (Peimbert 1967; Lee 1968*a*).

* *Contributions from the Louisiana State University Observatory, No. 40.*

The cause of the excess flux in the hydrogen Balmer continuum and in the hydrogen lines (Kaler 1966, 1968) is currently in dispute. Peimbert (1967) has suggested that temperature fluctuations exist in a nebula and that the hydrogen radiations are being emitted at a low temperature in the neighborhood of 6000° K. The ratio of the flux density of the Balmer continuum to the $H\beta$ flux has in fact been used to measure a temperature for the hydrogen emitting region (Peimbert 1967; Lee 1968*a*). It is not clear, however, whether this so-called hydrogen temperature reflects a physically real situation or simply an incomplete understanding of recombination. As an example of the difficulties involved, Lee (1968*a*) derives an electron temperature of 4800° K for IC 418 from the ratio between the Balmer continuum and $H\beta$ whereas LeMarne and Shaver (1969) obtain 12500° K from the radio continuum and Wilson and Aller's (1951) hydrogen intensity profile. Cahn and Kaler (1971) show, however, that in order to obtain realistic extinction coefficients the low hydrogen temperatures must be adopted whether or not they are physically real.

We now have an opportunity to measure other "temperatures" by using a different ion, and to measure helium-to-hydrogen ratios in a different way. We discuss the observations in § II and try to relate them to theory in § III.

II. THE OBSERVATIONS

The observations consist of the long-exposure plates used for the studies listed in Table 1, from which transmission tracings were made. We converted the transmission tracings to arbitrary intensity units over the region $3550\text{--}3300 \text{ \AA}$, and to correct the intensities to outside the atmosphere we used the reduction procedures described in the papers listed in Table 1. We then corrected for interstellar reddening, where we used the reddening function given by Seaton (1960) and the reddening constants listed in column (2) of Table 3 which are from Kaler (1970). The spectral range given above is large enough to establish the continua on either side of the 2^3P series limit, and thus to allow us to measure the intensity of the 2^3P continuum at the limit. No attempt has been made to incorporate recent calibrations of standard stars (e.g., Hayes 1970) because of the uncertainty of the results described herein and because of the insensitivity of the results to any required changes in the calibrations.

We give an example of the observations in Figure 1. This figure shows the transmission tracing of plate Ce 12791 of NGC 6572, which exhibits the most pronounced effect of the continuum. Note that the increase in intensity occurs at $\lambda 3440$, which corresponds to the confluence of the helium lines at about $n = 30$. The individual lines themselves disappear into the plate noise at about $n = 20$. The "quasicontinuum" between $\lambda\lambda 3440$ and 3422 is actually due to the confluence of *two* series of lines. The observed lines of the

TABLE 1
THE SOURCE OF THE OBSERVATIONS, AND THEIR REFERENCES

Nebula	Plate	Telescope	References
IC 418	EC 2438	Lick 120-inch coudé	Aller and Kaler (1964 <i>b</i>)
IC 4997 (1)	Ce 14769	Mount Wilson 100-inch coudé	Aller and Kaler (1964 <i>c</i>)
IC 4997 (2)	Ce 12790		
Orion Nebula	EC 2693	Lick 120-inch coudé	Kaler, Aller, and Bowen (1965)
NGC 6543	C 44	KPNO 84-inch Cassegrain	Czyzak, Aller, and Kaler (1968)
NGC 6572	Ce 12791	Mount Wilson 100-inch coudé	Aller and Kaler (1964 <i>c</i>)
NGC 7009	Ce 14767	Mount Wilson 100-inch coudé	Aller and Kaler (1964 <i>a</i>)
NGC 7662	Ce 14765	Mount Wilson 100-inch coudé	Aller, Kaler, and Bowen (1966)
θ Cr	EC 2694	Lick 120-inch coudé	
BD+28°4211	EC 2437	Lick 120-inch coudé	

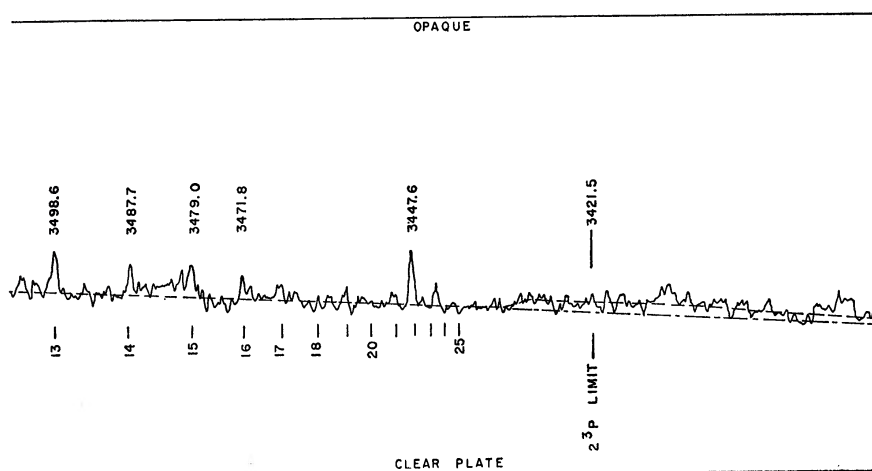


FIG. 1.—Microphotometer tracing of plate number Ce 12791 of NGC 6572. The number of the upper quantum level of the 2^3P-n^3D series is marked at the expected position of the line. The wavelengths of several helium lines are also given. (The He I (2^1S-6^1P) $\lambda 3447.6$ line is not part of the series.) *Dashed line*, continuum; long and short dashes represent the extension of the Balmer continuum shortward of the helium series limit.

2^3P-n^3S series have generally only about 10 percent of the intensities of the 2^3P-n^3D lines, so that because of the low signal-to-noise ratio the 2^3P-n^3S series is inconsequential.

The reduced flux densities of the continuum, on an arbitrary scale, are given in Figure 2. We see that in most cases the rise in the continuum level is only a little greater than the variations introduced by the plate itself. The fact that the increase occurs at nearly the same wavelength for *all* nebulae demonstrates that we are dealing with a real effect and not an effect of noise. Note that the observations were made with three instruments: the Mount Wilson 100-inch coudé, the Lick 120-inch coudé, and the Kitt Peak 84-inch Cassegrain spectrographs, which would indicate that the feature is real in the nebula and not an effect of the spectrograph. In addition, coudé spectrograms of θ Crt and BD+28°4211 (which were used as standard stars for the data on the Orion Nebula and IC 418, respectively) taken with the 120-inch telescope were reduced in the same manner as the nebulae. These observations are plotted in Figure 3; neither of these stars shows any trace of a rise in the neighborhood of $\lambda 3440$.

We have one nebula (IC 4997) for which we have two plates of comparable quality. Note that the rise begins at a somewhat longer wavelength for IC 4997 than for the other nebulae, and it does so on both plates.

The plate of NGC 7662 was traced on either side of the central star. The 2^3P continuum is detected and measured on both tracings, but only the better of the two (No. 2 in Tables 3 and 4) is represented in Figure 2.

These facts and the nature of the rise would appear to eliminate nightsky radiation as the cause of the observations.

Where possible, tests of a statistical nature have been applied to the data on the helium continuum. The four tests, not all of which have been applied to each set of data, are: (1) runs above and below the mean, (2) runs up and down, (3) a χ^2 test, and (4) a Kolmogorov-Smirnov test. At all times the observations have been treated as though they represented a statistical distribution, an assumption which is not strictly true. Nevertheless, the results should permit one to assess the reality and significance of the feature in question. The procedure has been as follows. The wavelength dependence of the continuum resulting from a free-bound process is small over an interval

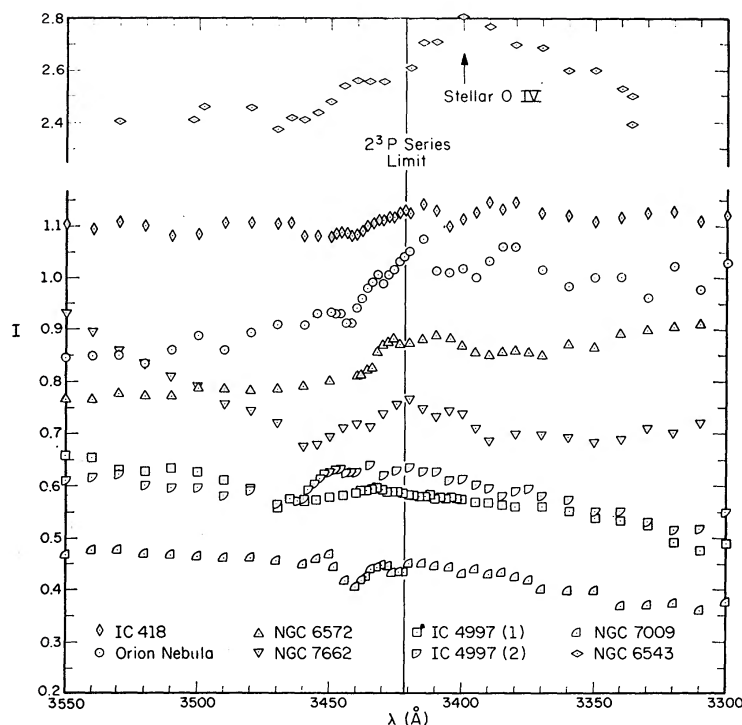


FIG. 2.—Reduced continua for several nebulae on an arbitrary scale. *Vertical line*, true series limit.

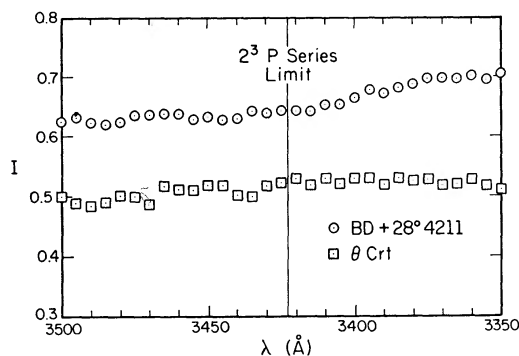


FIG. 3.—Reduced continua for two comparison stars on an arbitrary scale. *Vertical line*, helium series limit.

of 200 Å. Thus, a baseline was drawn in by eye estimate longward of the limit 3421.5 Å and a line parallel to the first was drawn through the points to shorter wavelengths. Ordinates were then measured perpendicular to these lines. The slope of these two lines with respect to wavelength was considered of no importance because of possible systematic errors and central-star contamination. Tests 1 and 2 have been applied to the points in Figure 2 at 10 Å intervals over the range 3500–3300 Å. The hypothesis that we investigate by tests 3 and 4 is that the data points in Figure 2 are described by a suitably synthesized pseudocontinuum (see § III). The electron temperature was chosen so that the free-bound continuum of helium would be of the observed intensity. The points selected for the χ^2 test were between 3450 and 3420 Å in 5 Å intervals. For both

tests 3 and 4 the computed intensities of the unobserved lines were averaged out over the interval between the lines; such a procedure will maximize χ^2 . The results are given in Table 2.

Two problems in the observation of the 2^3P continuum should be mentioned. For many of the small planetary nebulae it is very difficult to avoid contamination by the central star. In the case of NGC 6543 (Fig. 2), this contamination causes stellar O IV lines to be superimposed on the spectrum in the region 3400–3423 Å. The problems of observation are quite difficult for the high-excitation nebulae, as the strong nebular lines $\lambda\lambda 3412, 3422, 3444$ of O III and $\lambda 3425$ of [Ne V] are in the region of interest. These lines are responsible for lower accuracies for NGC 7662 and NGC 7009.

For comparison with recombination theory, we have measured the ratio of the 2^3P flux density to both the flux in the $\lambda 4471$ line of He I and the flux density of the Balmer continuum at $\lambda 3646$. The former ratio is dependent only upon electron temperature, while for an isothermal nebula the latter depends only on the ratio of singly ionized helium to hydrogen.

We define the ratio

$$\rho = F_\lambda(2^3P) \text{ \AA}^{-1} / F(\lambda 4471), \quad (1)$$

where $F_\lambda(2^3P)$ is the flux in 1 Å of the 2^3P continuum at the series limit and $F(\lambda 4471)$ is the flux in the $\lambda 4471$ line. Generally, $\lambda 4471$ is not observed on the same plate as the 2^3P continuum, so that one or more of the lines which are $\lambda\lambda 3587, 3634, 4009$, etc., must be used for interpolation. We use the intensities given in the references of Table 1.

In Figure 2, let I_b and I_r be the intensities of the nebular continuum on the blue and red side of the series limit. Then

$$F_\lambda(2^3P) = (I_b - I_r) / D, \quad (2)$$

where D is the apparent dispersion on the tracing in Å cm^{-1} . We then measure the area under (for example) the line $\lambda 3634$ which appears on the same tracing, and apply the same reduction procedure that we used to get the continuum intensity. We now have the flux of the $\lambda 3634$ line in the same arbitrary units as $F_\lambda(2^3P)$. Then,

$$\rho = \frac{F(2^3P) I(3634)}{F(3634) I(4471)}, \quad (3)$$

where the ratio $I(3634)/I(4471)$ is obtained from the appropriate reference of Table 1—all this after correction for interstellar reddening. Lines other than $\lambda 3634$ are often used. The values of ρ which we derive are of course very dependent upon the exact placement of the continuum in Figure 2. We make as many as three types of measurements: the most likely (as it appears to us), the minimum, and the maximum allowable

TABLE 2
LEVEL OF SIGNIFICANCE

Object	Test 1 (Percent)	Test 2 (Percent)	Test 3 (Percent)	Test 4 (Percent)
IC 418.....	1	20	5	20
IC 4997 (2).....	1	1	2	20
NGC 1976.....	1	5	1	20
NGC 6543.....	1	5
NGC 6572.....	1	1	5	20
NGC 7009.....	5	Random
NGC 7662.....	1	5

values of $F_\lambda(2P^3)$. The most likely, or adopted, value was obtained by simply passing the best mean line through the points longward and shortward of the 2^3P limit. For the "minimum" measurements, where they apply, we gave high weight to those observed points which tended to minimize the continuum height. For several nebulae, up to three different lines were used for the interpolation; error introduced by this procedure is not likely to exceed ± 20 percent. The measurements of ρ are presented in Table 3. Column one gives the nebula, column (2) the adopted reddening constant from Kaler (1970) and columns (3), (4), and (5) give the various values of ρ .

Next, we form the ratio

$$\sigma = \frac{F_\lambda(2^3P) \text{ \AA}^{-1}}{F_\lambda(\text{Bac}) \text{ \AA}^{-1}}, \quad (4)$$

where $F_\lambda(\text{Bac})$ is the flux in 1 \AA of the Balmer continuum at the series limit. This ratio can be found with no interpolation, because both continua appear well exposed on the same plate. A distinct advantage to the use of this ratio is that the wavelength difference between the two continua is small and errors in the correction to outside the atmosphere and interstellar reddening will also be small. The observed values of σ are presented in Table 3 in columns 6, 7, and 8. The last five columns are discussed in the next section.

III. DISCUSSION

We would like to compare the observed values of ρ and σ with those derived from recombination theory. According to Brown and Mathews (1970) the energy in any continuum per unit time and volume can be written as

$$\epsilon_\nu = N_i N_e \gamma d\nu, \quad (5)$$

where γ is the emission coefficient and N_i and N_e are the ion and electron densities, respectively. The emissivity in the $\lambda 4471$ line can be written as

$$\epsilon(\lambda 4471) = N_i N_e a_{4d,2p}(\text{He}) h\nu, \quad (6)$$

where $a_{4d,2p}$ is the effective recombination coefficient for the $\lambda 4471$ line (Seaton 1960). We can then express the theoretical ratios of ρ and σ as

$$\rho_T = \frac{\epsilon_\lambda(2^3P)}{\epsilon(\lambda 4471)} = 5.76 \times 10^{22} \frac{\gamma_\nu(2^3P)}{a_{4d,2p}} \quad (7)$$

and

$$\sigma_T = \frac{\epsilon_\lambda(2^3P)}{\epsilon_\lambda(\text{Bac})} = 1.075 \frac{\gamma_\nu(2^3P) \text{ He}^+}{\gamma_\nu(\text{Bac}) \text{ H}^+}. \quad (8)$$

We compute values of ρ_T and σ_T for each nebula, where we use the electron temperatures computed from the [O III] line intensities and the He^+/H^+ ratios, both from Kaler (1970). Values of $\gamma_\nu(2^3P)$ and $\gamma_\nu(\text{Bac})$ are taken from Brown and Mathews (1970), and values of $a_{4d,2p}$ are from Pengelly (private communication). The electron temperatures (called $T_e(F)$), the He^+/H^+ ratio, and the resulting values of ρ_T and σ_T are presented in columns (9), (10), (11), and (12) of Table 3. Columns (13) and (14) then give

$$R = \rho/\rho_T \quad \text{and} \quad \Sigma = \sigma/\sigma_T. \quad (9)$$

Note that in all but one case $\rho > \rho_T$ and $\sigma > \sigma_T$, often by substantial amounts. The 2^3P continuum is too strong both as compared with $\lambda 4471$ and as compared with the Balmer continuum, in the same sense as the Balmer continuum is too strong when compared with $\text{H}\beta$ (see, e.g., Lee 1968*a*), at the electron temperature found from the forbidden lines.

We can use equations (7) and (8) to determine the parameters necessary to fit the

TABLE 3
STRENGTH OF THE HELIUM 2³P CONTINUUM COMPARED WITH THOSE OF $\lambda 4471$ AND THE BALMER CONTINUUM

Nebula (1)	c (2)	ρ_{adopt} (3)	ρ_{min} (4)	ρ_{max} (5)	σ_{adopt} (6)	σ_{min} (7)	σ_{max} (8)	T_e (F) ($^{\circ}$ K) (9)	He ⁺ /H (10)	ρ_T (11)	σ_T (12)	R (13)	Σ (14)
IC 418.....	0.33	0.0125	0.0087	...	0.074	0.051	...	11000	0.064	0.0078	0.055	1.6	1.3
IC 4997 (1).....	0.54	0.0087	0.0066	...	0.137	0.105	...	18800	0.139	0.0061	0.120	1.4	1.1
IC 4997 (2).....	0.54	0.0098	0.173	18800	0.139	0.0061	0.120	1.6	1.4
NGC 6543.....	0.22	0.0153	0.113	8200	0.110	0.0087	0.095	1.8	1.2
NGC 6572.....	0.31	0.0253	0.0192	...	0.176	0.134	...	10500	0.102	0.0079	0.088	3.2	2.0
NGC 7009.....	0.24	0.0048	...	0.0132	0.041	...	0.113	10600	0.122	0.0079	0.105	0.6	0.4
NGC 7662 (1).....	0.40	0.0244	0.152	13000	0.065	0.0072	0.056	3.4	2.7
NGC 7662 (2).....	0.40	0.0166	0.0106	...	0.158	0.110	...	13000	0.065	0.0072	0.056	2.3	2.8
Orion Nebula.....	0.36	0.0304	0.0237	...	0.180	0.140	...	9200	0.101	0.0083	0.087	3.7	2.1

theory to the observations. From equation (7) we derive a temperature from the ratio of the strengths of the 2^3P continuum and $\lambda 4471$. These temperatures (called $T_e(\text{He I})$) are presented in columns (2), (3), and (4) of Table 4, where they correspond to the various values of ρ .

We may also use the profile of the confluence of the lines between $\lambda\lambda 3440$ and 3421 to arrive at electron temperatures, as Lee (1968*b*) has done for the Balmer confluence. We adopt a mean profile from observable lines and then compute the profile of the confluence from an expected run of b_n (departures from thermal equilibrium) as computed by Clarke (1965) and Seaton (1964). We then compute what electron temperature is needed to give the observed intensity of the quasicontinuum of the line confluence at the position of $n = 100$. These temperatures, denoted by $T_e(\text{line})$, should be similar to those from the continuum and are presented in column (5) of Table 4 rounded to the nearest 500°K . For comparison we give the electron temperatures computed by Lee (1968*a*) from the hydrogen Balmer continuum, and those computed by Kaler (1968) from the Balmer decrement in columns (6) and (7) of Table 4.

Note the very low values of the "helium temperatures" which in many cases lie substantially below even the analogous "hydrogen temperatures."

The values of He^+/H^+ needed to fit the ratio of the 2^3P continuum strength to that of the Balmer continuum for an isothermal nebula are given in column (8) of Table 4 as He^+/H^+ (1). They are nearly all greater than the He^+/H^+ ratios found from the ratio of fluxes of $\lambda 4471$ to $\text{H}\beta$ as given in Table 3. This is, of course, consistent with $T_e(\text{He I}) < T_e(\text{H})$.

If these temperatures are physically real, or if we simply allow them as a fitting parameter, we should be able to use $T_e(\text{He I})$ and $T_e(\text{H})$ to compute $\gamma(2^3P)$ and $\gamma(\text{Bac})$, respectively, and thereby derive the correct helium-to-hydrogen ratio. Values calculated by this procedure are given in column (9) of Table 4 as He^+/H^+ (2). He^+/H^+ (2) ratios for IC 418, IC 4997, and NGC 6543 are certainly acceptable, but those for NGC 6572, NGC 7662, and the Orion Nebula are much too low.

It should be kept in mind that individual values are subject to large error. In particular, the observations of NGC 7009 and NGC 7662 are quite unreliable because of overlying high-excitation nebular lines; the 2^3P continuum for these two nebulae should be regarded as a detection only. *What is significant here is the consistency of the observations for the low excitation nebulae.* The observed strength of the 2^3P continuum is too high for all of these nebulae.

In conclusion, it seems safe to assume that the 2^3P continuum can be regarded as detected, and that it shares, with the hydrogen continuum, an anomalously high

TABLE 4
ELECTRON TEMPERATURES AND He^+/H^+ RATIOS DERIVED
FROM DATA ON THE HELIUM CONTINUUM

Nebula (1)	Adopted	max	min	$T_e(\text{line})$ ($^\circ \text{K}$) (5)	$T_e(\text{Bac})$ ($^\circ \text{K}$) (6)	$T_e(\text{dec})$ ($^\circ \text{K}$) (7)	He^+/H^+ (1) (8)	He^+/H^+ (2) (9)
	$T_e(\text{He I})$ ($^\circ \text{K}$) (2)	$T_e(\text{He I})$ ($^\circ \text{K}$) (3)	$T_e(\text{He I})$ ($^\circ \text{K}$) (4)					
IC 418.....	4100	8200	...	2000	4800	2500	0.09	0.07
IC 4997.....	7100	15000	...	3500	12000	8000	0.17	0.10
NGC 6543.....	2800	3700	9000	0.13	0.09
NGC 6572.....	1400	2000	...	3000	6100	5000	0.20	0.02
NGC 7009.....	>10000	...	3700	...	9700	...	0.05	...
NGC 7662 (1).....	1500	5800	8000	0.18	0.04
NGC 7662 (2).....	2500	5800	8000	0.18	0.04
Orion Nebula.....	~ 1000	1500	...	~1500	4700	1250	0.21	0.04

strength. In addition, it seems likely that this effect is even greater for helium than for hydrogen. The results argue against the effect being due solely to a low temperature, although temperature effects may account for some of the problem. If the nebulae were radiating properly at $T_e(F)$, we would not have detected the helium continuum at all.

It is clear that the 2^3P continuum needs further observations with a substantially higher signal-to-noise ratio; the problem should be attacked photoelectrically.

We would like to thank Mr. Victor Broquard for assistance in the reductions, Dr. J. Dickel for helpful comments on the manuscript, and Dr. William G. Mathews for communicating the theoretical helium data in advance of publication. This work was supported by the National Science Foundation under grants GP 4928 and GP 7816 to the University of Illinois and by the Air Force Office of Scientific Research, Office of Aerospace Research, U.S. Air Force, under grant 83-67 to the University of California, Los Angeles. One of us (P. L.) was supported by a NASA Traineeship at the University of Illinois during part of the work. We would also like to thank Mount Wilson and Palomar Observatories, and the Kitt Peak National Observatory, where some of the observations were made.

REFERENCES

- Aller, L. H. 1956, *Gaseous Nebulae* (New York: John Wiley & Sons)
 Aller, L. H., and Kaler, J. B. 1964a, *A p. J.*, **139**, 1074.
 ———. 1964b, *ibid.*, **140**, 936.
 ———. 1964c, *ibid.*, p. 621.
 Aller, L. H., Kaler, J. B., and Bowen, I. S. 1966, *A p. J.*, **144**, 291.
 Bethe, H. A. 1964, *Intermediate Quantum Mechanics* (New York: W. A. Benjamin, Inc.).
 Brown, R. L., and Mathews, W. G. 1970, *A p. J.*, **160**, 939
 Cahn, J. H., and Kaler, J. B. 1971, *A p. J. Suppl.* (in press)
 Clarke, W. H. 1965, unpublished thesis, University of California, Los Angeles.
 Czyzak, S. J., Aller, L. H., and Kaler, J. B. 1968, *A p. J.*, **154**, 543.
 Hayes, D. S. 1970, *A p. J.*, **159**, 165.
 Kaler, J. B. 1966, *A p. J.*, **143**, 722.
 ———. 1968, *A p. Letters*, **1**, 227.
 ———. 1970, *A p. J.*, **160**, 887.
 Kaler, J. B., Aller, L. H., and Bowen, I. S. 1965, *A p. J.*, **141**, 912.
 LeMarne, A. E., and Shaver, P. A. 1969, *Proc. Astr. Soc. Aust.*, **1**, 216.
 Lee, P. 1968a, *A p. Letters*, **1**, 225.
 ———. 1968b, unpublished thesis, University of Illinois.
 Peimbert, M. 1967, *A p. J.*, **150**, 825.
 Seaton, M. J. 1960, *Rept. Progr. Phys.*, **23**, 313.
 ———. 1964, *M.N.R.A.S.*, **127**, 177
 Wilson, O. C., and Aller, L. H. 1951, *A p. J.*, **114**, 121.

